Solid-State Electronics 185 (2021) 108040

Contents lists available at ScienceDirect

Solid State Electronics

journal homepage: www.elsevier.com/locate/sse

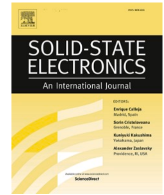

SPICE modeling of cycle-to-cycle variability in RRAM devices

E. Salvador [a,*], M.B. Gonzalez [b], F. Campabadal [b], J. Martin-Martinez [a], R. Rodriguez [a], E. Miranda [a]

[a] *Departament d'Enginyeria Electrònica, Universitat Autònoma de Barcelona, 08193 Cerdanyola del Valles, Spain*
[b] *Institut de Microelectrònica de Barcelona, IMB-CNM, CSIC, 08193 Cerdanyola del Valles, Spain*

ARTICLE INFO

Keywords:
RRAM
Variability
Modeling
LTSpice
Fitdistrplus

ABSTRACT

In this work, we investigated how to include uncorrelated cycle-to-cycle (C2C) variability in the LTSpice quasi-static memdiode model for RRAM devices. Variability in the I-V curves is first addressed through an in-depth study of the experimental data using the *fitdistrplus* package for the R language. This provides a first approximation to the identification of the most suitable model parameter distributions. Next, the selected candidate distributions are incorporated into the model script and used for carrying out Monte Carlo simulations. Finally, the experimental and simulated observables (set and reset currents, transition voltages, etc.) are statistically compared and the model estimands recalculated if it is necessary. Here, we put special emphasis on describing the main difficulties behind this seemingly simple procedure.

1. Introduction

Memristors or Resistive RAMs (RRAMs) are electroformed metal-oxide-metal devices that can alter their resistance states in a non-volatile fashion. They are currently considered not only for memory arrays but also for a plethora of applications including neuromorphic computing, logic circuits, cryptography, etc. [1–3]. Nevertheless, one of the major drawbacks that this technology currently faces concerns with its inherent variability, which is associated with the alternate formation and destruction of the filamentary conducting structure at atomic scale [4,5]. Since variability is at the heart of RRAM operation, inclusion of this phenomenon in any compact model intended for circuit simulation environments would be of utmost importance. In this work, we explore the introduction of uncorrelated cycle-to-cycle (C2C) variability in the quasi-static memdiode model (QMM) for RRAM devices [6]. Correlated C2C variability involving time series dependence (simulation results for cycle *i* depend on simulation results for cycle *i-1*) and chained parameter simulations involving multivariate regression (parameter value *i* explicitly depends on parameter value *j* within cycle *k*) are the following logical steps to investigate after this first attempt. However, before entering into the subject, it is important to understand how variability affects the simulation results. Uncorrelated C2C variability does not mean that the parameter estimands can be independently chosen within a certain cycle. Since the generated *I-V* curve is the result of a sequence of operations in which multiple parameters intervene, there is an underlying connection among their average and dispersion values. This interdependence must be addressed in order to obtain realistic simulated curves. In this work, we adopt a simplistic approach which consists in estimating first the most suitable distribution functions for the experimental observables and then attributing these functions to the corresponding most relevant model parameters in each part of the *I-V* curve. However, recall that the final simulated curve is the result of a combination of nonlinear functions with random parameters. In order to obtain acceptable results under this scheme, we follow a kind of recursive approach in which the model parameters are at the end selected according to the statistical results they generate.

2. Devices and experimental results

HfO_2-based MIM structures [7] were investigated in this work. The oxide thickness is 10 nm and the area of the devices 5x5μm^2. The bottom electrode is a 200 nm-thick W layer and the top electrode is a 200 nm-thick TiN layer on top of a 10 nm-thick Ti layer acting as oxygen getter material [8]. Simulations are compared with experimental data obtained from applying 450 voltage sweeps to the devices described previously. The complete set of experimental *I-V* curves and the median curve are shown in Fig. 1.a. High (I_{HRS}) and low (I_{LRS}) resistance state currents are extracted at $V = 0.2$ V. The snapback (SB) correction is calculated as $V_{SB} = V_{applied} - R_i \cdot I_{measured}$, where R_i is a series resistance (internal). R_i is chosen so as to achieve a current increase at a constant

* Corresponding author.
E-mail address: emili.salvador@uab.cat (E. Salvador).

https://doi.org/10.1016/j.sse.2021.108040

Available online 29 May 2021
0038-1101/© 2021 The Author(s). Published by Elsevier Ltd. This is an open access article under the CC BY license (http://creativecommons.org/licenses/by/4.0/).

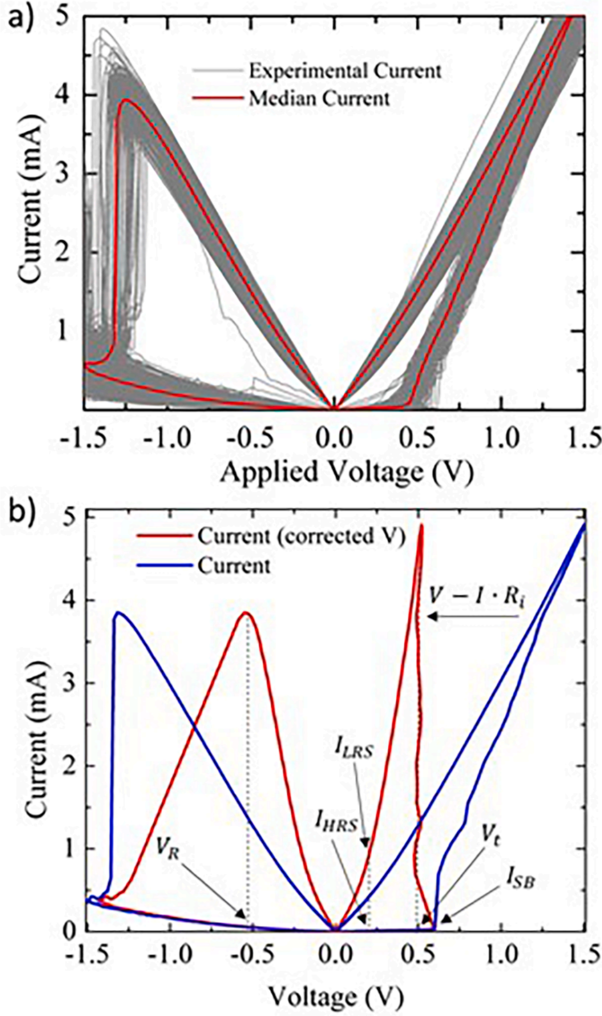

Fig. 1. a) Experimental I-V curves: 450 cycles and median curve. b) Voltage correction illustrating the snapback effect in a single cycle and parameter specification.

transition voltage V_T (see Fig. 1.b) [9]. This correction is calculated for all the cycles using a different R_i value. The RESET voltage V_R is the voltage corresponding to the maximum current reached at negative bias. The SB current I_{SB} is found from the last data point before the occurrence of the SET jump. The parameter extraction was carried out using MATLAB. The extracted parameters for the whole set of curves were analyzed using the tools available in the *fitdistrplus* package for the R language [10]. Different distributions (normal, lognormal, gamma, and Weibull) were fitted to the data and compared. The goodness of fit and criteria (minimum values in Table 1) in combination with the quantile–quantile (Q-Q) plots are illustrated in Fig. 2, which graphically compare the experimental distributions with the parametric models. This information is used to determine the best candidate distributions.

Fig. 2.a, .b and .c show the density plots for V_T, V_R and R_i corresponding to the four distributions investigated. According to this analysis, V_T follows a lognormal distribution while V_R and R_i are better described by a normal one. The same analysis was carried out for the rest of the above mentioned parameters resulting in: normal distribution for I_{SB}, and lognormal distributions for I_{HRS} and I_{LRS}. This prior information will be used to define the distribution of the leading model parameters in the device script.

Table 1
Goodness-of-fit statistics (Kolmogorov-Smirnov, Cramer-von Mises, Anderson-Darling) and criteria (Akaike's and Bayesian) for a) V_T, b) for V_R and c) for R_I.

a)

	Method	Normal	Lognormal	Gamma	Weibull
Stat.	K-S	0.0375	**0.0295**	0.0298	0.0856
	C-vM	0.1289	**0.0576**	0.0696	0.9333
	A-D	0.9495	**0.3944**	0.5076	6.343
Cri.	AIC	-1654.55	**-1662.72**	-1661.04	-1585.18
	BIC	-1646.34	**-1654.501**	-1652.82	-1576.96

b).

	Method	Normal	Lognormal	Gamma	Weibull
Stat.	K-S	**0.0275**	0.0449	0.0393	0.046
	C-vM	**0.045**	0.1709	0.1149	0.2497
	A-D	**0.2707**	1.043	0.6944	1.858
Cri.	AIC	**-1500.53**	-1487.75	-1493.46	-1480.1
	BIC	**-1492.32**	-1479.532	-1485.25	-1471.89

c).

	Method	Normal	Lognormal	Gamma	Weibull
Stat.	K-S	**0.0954**	0.0986	0.1003	0.1532
	C-vM	**0.7561**	0.7826	0.8059	3.077
	A-D	**4.819**	4.991	5.137	18.919
Cri.	AIC	**-3315.67**	-3313.39	-3313.25	-3463.92
	BIC	**-3323.89**	-3321.62	-3321.46	-3472.14

3. QMM with variability

Once the model parameter distributions are established, they are included in the header of the QMM model script as shown in Table 2. Some model parameters are assumed to be constant in order to avoid over-randomness. The LTSpice *gauss* function and its transformations are used to generate the appropriate parameter values and variability. According to the QMM [2] the *I-V* characteristic reads:

$$I(V) = I_0(\lambda) sinh\{\alpha(\lambda)[V - (R_S(\lambda) + R_i)I]\} \quad (1)$$

where $I_0(\lambda) = I_{omin} + (I_{omax} - I_{omin})\cdot\lambda$ is the current amplitude factor, R_S a series resistance, α a fitting parameter and I_{omin} and I_{omax}, minimum and maximum current values, respectively. Equation (2) relates the memory state λ to the voltage across the filament's constriction V_C through the recursive hysteresis operator:

$$\lambda(V_C) = min\left\{\Gamma^-(V_C), max\left[\lambda(\overleftarrow{V_C}), \Gamma^+(V_C)\right]\right\} \quad (2)$$

where Γ^+ and Γ^- are the so-called ridge functions, which represent the ion/vacancy movement for SET and RESET, respectively. $\lambda\left(\overleftarrow{V_C}\right)$ is the memory value a timestep before (dictated by the simulator). The model includes other parameters for the fine-tuning of the simulated curves.

4. Comparison between experimental and simulation results

The next step consists in performing Monte Carlo simulations using the QMM model discussed in the previous Section. In Fig. 3, experimental (grey) and simulated (red) curves are compared using three

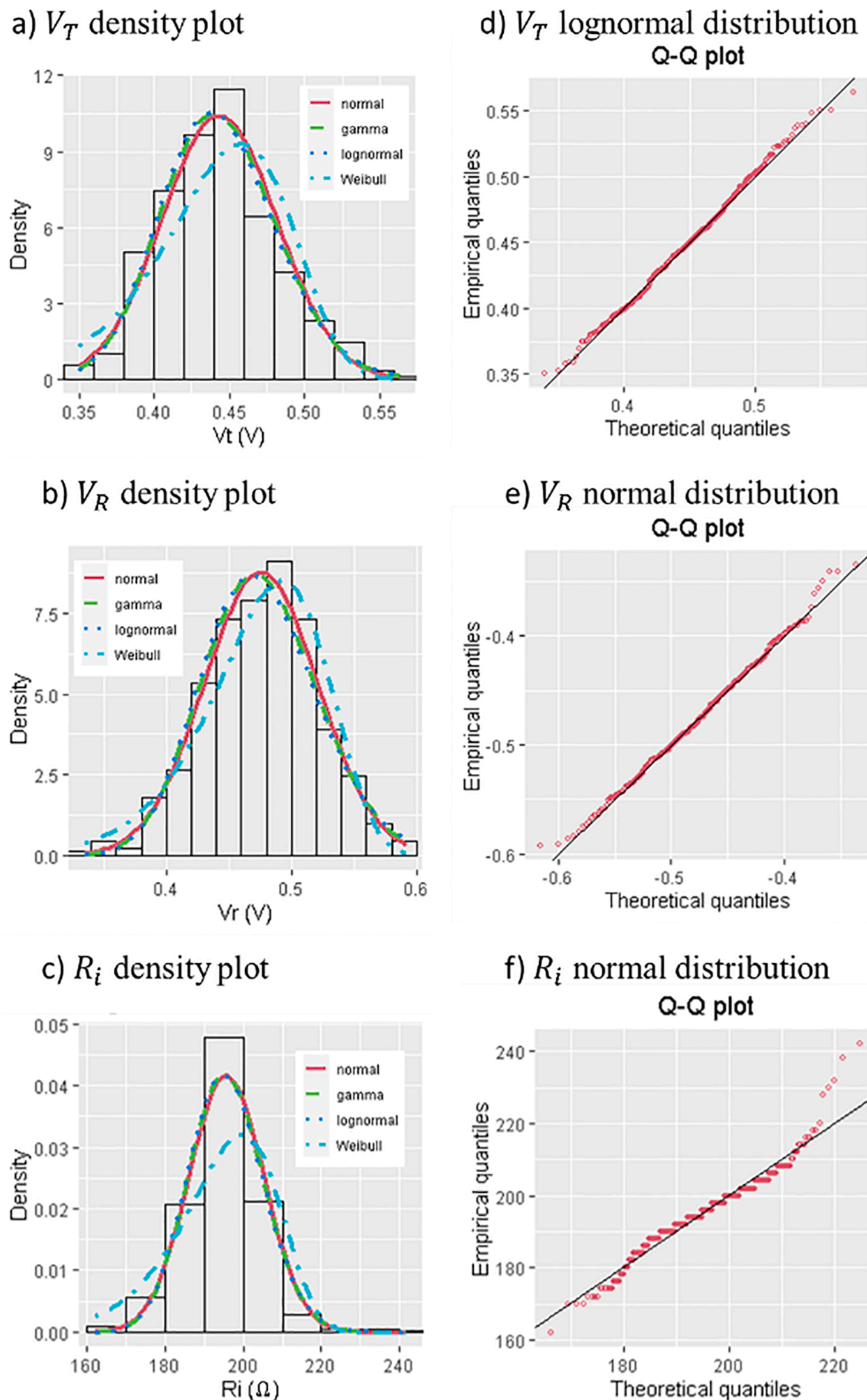

Fig. 2. a), b) and c) show density plots for V_T, V_R and R_i, respectively, with normal, gamma, lognormal, and Weibull distributions. d), e) and f) show Q-Q plots after selecting the best fitting distribution.

different plots for the *I-V* curves: *a)* linear–linear, *b)* log-linear, and *c)* linear–linear (with SB correction). Although the fitting is not perfect, the simulations reproduce the main features of the experimental curves in all the cases. The most conspicuous difference occurs in LRS, mainly because of a peculiarity of the experimental data. This will be discussed in detail next.

In order to make a fair comparison, the statistical distributions of the four observables is considered in Fig. 4. These observables were specifically selected so as to compile information from the entire set of the *I-V* curves in the different regimes: I_{HRS} for the HRS curve, V_T for the SET transition, I_{LRS} for the LRS curve and V_R for the RESET transition. This compilation was performed without considering the SB correction and for a direct evaluation of I_{HRS} and I_{LRS}. As shown in Fig. 4, simulation results for I_{HRS}, V_T, and V_R are consistent with the experimental data. However, I_{LRS} exhibits a notorious discrepancy. The reason is clear, for the particular case under study, the experimental I_{LRS} histogram presents

Table 2
LTSpice QMM script including variability in the most significant parameters taking into account the previously extracted best candidate distributions. In red the Gaussian distribution and in blue the lognormal distributions.

```
.subckt memdiode + - H
.params
+ H0=2E-3 ri=193+gauss(1)
+ etas=50 vs=2 etar=9 vr=-0.57+gauss(0.028)
+ rsmax=8+gauss(1) rsmin=10
+ imax=exp(-5.38+gauss(0.06)) amax=2.0
+ imin=exp(-10.9+gauss(0.68)) amin=2.0
+ vt=exp(-0.733+gauss(0.08)) isb=33E-6+gauss(2E-6)
+ CH0=1E-3 gam=0.07 RPP=1E10
*Memory equation
BH 0 H I=min(R(V(C,-)),max(S(V(C,-)),V(H))) Rpar=1
CH H 0 {CH0} ic={H0}
*I-V
RE + C {ri}
RS C B R=RS(V(H))
BD B - I=I0(V(H))*sinh(A(V(H))*V(B,-))
RB + - {RPP}
*Auxiliary functions
.func I0(x)=imin+(imax-imin)*x
.func A(x)=amin+(amax-amin)*x
.func RS(x)=rsmin+(rsmax-rsmin)*x
.func VSB(x)=if(x>isb,vt,vs)
.func ISF(x)=if(gam==0,1,pow(x,gam))
.func S(x)=1/(1+exp(-etas*(x-VSB(I(BD)))))
.func R(x)=1/(1+exp(-etar*ISF(V(H))*(x-vr)))
.ends
```

two peaks which likely corresponds to two different configurations of the filamentary path or to competing filaments. The simulated curves are unable to capture this feature because of the use of a single distribution function. This single distribution is responsible for the large central peak shown in Fig. 4.c. This inconsistency illustrates that caution should be exercised when unexpected deviations in the experimental data occur.

Finally, Fig. 5 illustrates the importance of C2C correlations in the experimental curves [11]. Experimental and simulated data corresponding to the time evolution of two parameters (high resistance state current I_{HRS} and reset voltage V_R) are compared. Notice that our approach is unable to generate a trend since the LTSpice simulations considered in this work are uncorrelated. These issues will be further investigated in the future.

5. Conclusions

In this work, we explored how uncorrelated C2C variability can be included in the QMM model for resistive switching devices. The experimental *I-V* curves obtained from HfO_2-based devices were analyzed and the main parameters extracted. The best candidate distributions for the experimental parameters were determined using the *fitdistrplus* package from the R language and this information was included in the model script. We showed that the model results reproduce reasonably well the

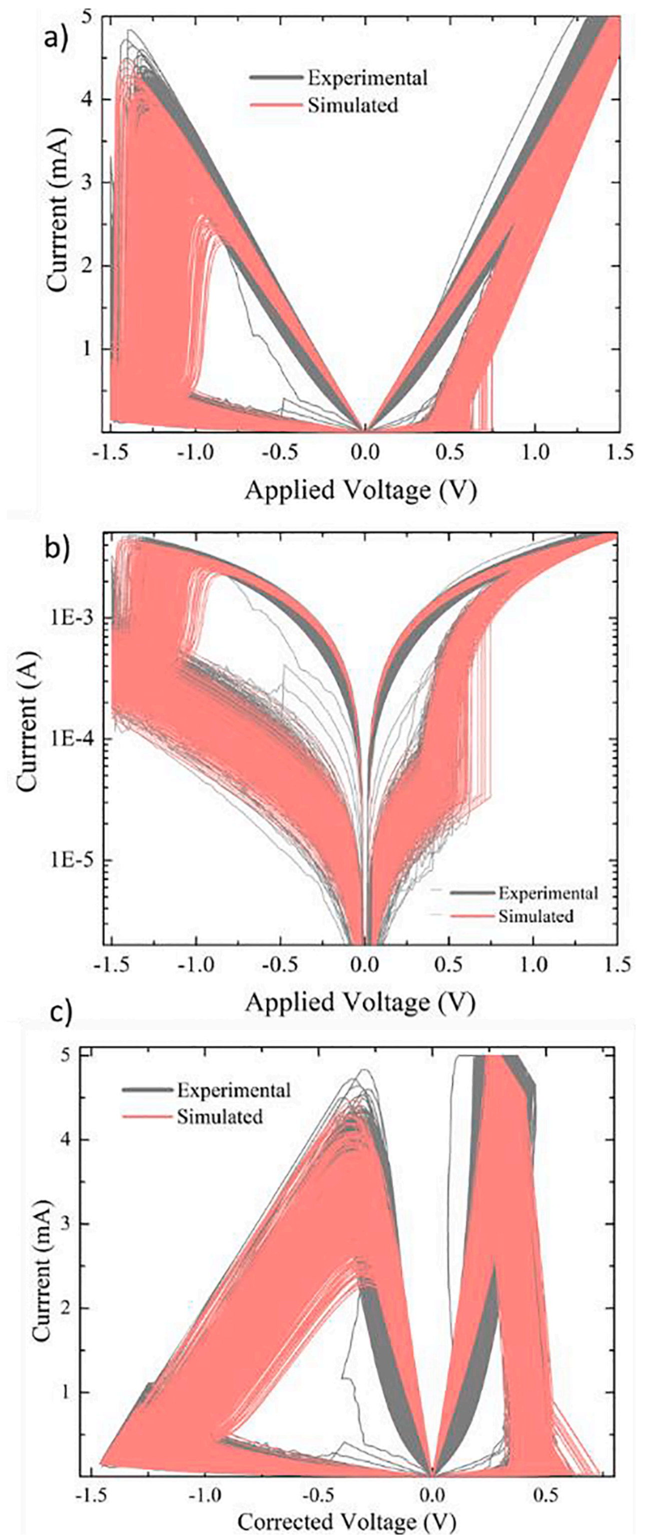

Fig. 3. Experimental and simulated curves comparison. a) I-V curves, b) I-V curves in logscale and c) I-V curves applying the SB voltage correction.

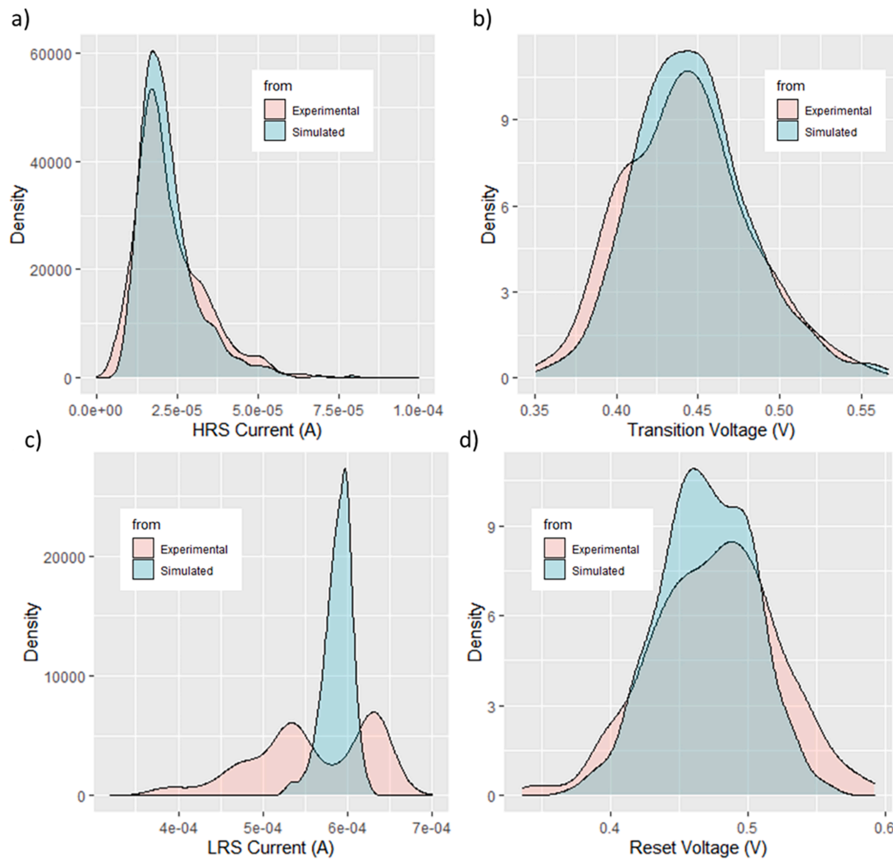

Fig. 4. Comparison of experimental and simulated parameter distributions: a)I_{HRS}, b) V_T, c)I_{LRS}, and d)V_R.

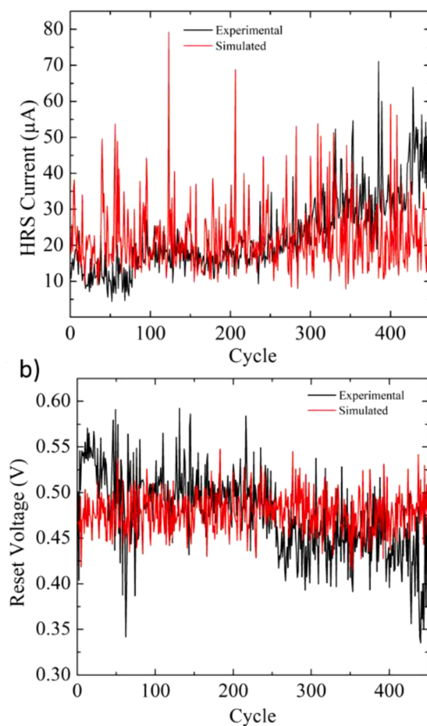

Fig. 5. Time evolution of experimental and simulated parameters for: a) HRS current and b) reset voltage.

main features exhibited by the experimental curves. Future investigations will include time series and chained-parameter analysis for correlated C2C variability simulations.

Declaration of Competing Interest

The authors declare that they have no known competing financial interests or personal relationships that could have appeared to influence the work reported in this paper.

Acknowledgements

This work was supported by the Spanish Ministry of Science, Innovation and Universities through projects TEC2017-84321-C4-1-R, TEC2017-84321-C4-4-R, and PID2019-103869RB-C32.

References

[1] Yu S, et al. IEEE Solid State Circuits Magazine 2016;8(2):43–56.
[2] Lee JS, Appl., et al. Phys. Rev. 2015;2(3):031303.
[3] Jo Sung Hyun, et al. Nano Lett 2010;10(4):1293–301.
[4] Chen A, et al. IEEE IRPS 2011;843–846.
[5] Bargallo M, et al. IEEE Trans. Electron Devices 2016;63(8):3116–22.
[6] Miranda E. IEEE TNano 2015;14:787–9.
[7] Piccolboni G, et al. IEEE Electron Device Lett. 2016;37(6):721–3.
[8] Poblador S, et al. Microelectron. Eng. 2018;187–188:148–53.
[9] Karpov V, et al. Appl. Phys. Lett. 2015;109:1–5.
[10] Delignette-Muller ML, et al. J. Stat. Softw. 2015;64:1–34.
[11] Alonso FJ, et al. Chaos. Solitons and Fractals 2021;143:110461.

Emili Salvador Aguilera is a PhD student at the Electronical Engineering department from the Universitat Autònoma de Barcelona under the supervision of Enrique Alberto Miranda and Rosana Rodríguez, from the same department. Prior to the PhD, coursed my Bachelor degree in Nanoscience and Nanotechnology and Master degree in Advanced Nanoscience and Nanotechnology at the Universitat Autònoma de Barcelona. He carried out my Master thesis at the Institut Català de Nanociència i Nanotechnology (ICN2) working in the graphene transistors field.

Mireia Bargallo Gonzalez received the degree in physics from the University of Barcelona, Barcelona, Spain, and the Ph.D. degree on the topic of stress analysis and defect characterization techniques of semiconductor materials and devices, from Katholieke Universiteit Leuven, Leuven, Belgium, in 2011. She pursued her Ph.D thesis with the Interuniversity Microelectronics Center (imec), Leuven, Belgium. In 2011, she joined the Institut de Microelectrònica de Barcelona (IMB-CNM, CSIC). Her current research interests include electrical characterization, modeling and applications of resistive switching devices.

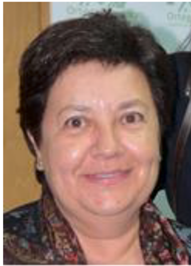

Francesca Campabadal received the Ph.D. degree in physics from the Universitat Autònoma de Barcelona, Bellaterra, Spain, in 1986. She joined the Institut de Microelectrònica de Barcelona, Consejo Superior de Investigaciones Científicas, Barcelona, Spain, in 1987, where she is currently a Research Professor. Her current research interests include the deposition of high-k dielectric layers, their electrical characteristics, and the resistive switching phenomena in RRAM devices.

Javier Martin-Martinez received the M.S. degree in physics from the Universidad de Zaragoza, Zaragoza, Spain, in 2004, and the Ph.D. degree from the Universitat Autònoma de Barcelona (UAB), Bellaterra, Spain, in 2009. He was with the Università degli Studi di Padova, Padua, Italy, and IMEC, Leuven, Belgium. He is currently an Associate Professor with UAB. His main research interests include the characterization and modeling of failure mechanisms in MOSFETs and also RRAM characterization and modeling for neuromorphic applications.

Rosana Rodriguez received the Ph. D. in Electrical Engineering from Universitat Autonoma de Barcelona (UAB) in 2000. Funded by the Fulbright program, she worked on devices and circuits reliability at the IBM Thomas J. Watson Research Center (USA). Currently, she is associate professor at the UAB. Her research is focused on the variability and reliability of advanced CMOS devices. She is interested in the electrical characterization and modeling of process-related and time–dependent variability sources as Random Telegraph Noise (RTN) and aging mechanisms as Bias Temperature instability (BTI) and Hot Carrier Injection (HCI). Her research includes the study of the variability impact on the performance of single devices and digital and analogical circuits. She is also interested in the characterization of resistive switching devices (memristors) and their application for non-volatile memories, computing and neuromorphic applications.

Enrique Miranda is Professor at the Universitat Autonoma de Barcelona (UAB), Spain. He has a PhD in Electronics Engineering from the UAB (1999) and a PhD in Physics from the Universidad de Buenos Aires, Argentina (2001). He received numerous scholarships and awards including: RAMON y CAJAL (UAB), DAAD (Technical University Hamburg-Harburg), MATSUMAE (Tokyo Institute of Technology, Japan), TAN CHIN TUAN (Nanyang Technological University, Singapore), WALTON award from Science Foundation Ireland (Tyndall National Institute), Distinguished Visitor Award (Royal Academy of Engineering, UK), CESAR MILSTEIN (CNEA, Argentina), Visiting Professorships from the Abdus Salam International Centre for Theoretical Physics, Slovak Academy of Sciences, Politecnico di Torino, Leverhulme Trust (University College London, UK), and Nokia Foundation (University of Turku, Finland). He serves as member of the Distinguished Lecturer program of the Electron Devices Society (EDS-IEEE) since 2001 and as Associate Editor of Microelectronics Reliability since 2003. He has authored and co-authored around 250 peer-review journal papers.